AI-Driven stress monitoring in melon crops via graph neural networks

Son Ali Akbar [a,1,*], Jihad Rahmawan [b,2], Etika Dyah Puspitasari [c,3], Anton Yudhana [a,4], Novi Febrianti [c,5]

[a] Department of Electrical Engineering, Universitas Ahmad Dahlan, Yogyakarta 55191, Indonesia
[b] Department of Informatics, Universitas Ahmad Dahlan, Yogyakarta 55191, Indonesia
[c] Department of Biology Education, Universitas Ahmad Dahlan, Yogyakarta 55191, Indonesia
[1] son.akbar@te.uad.ac.id; [2] jihad@tif.uad.ac.id; [3] etika.puspitasari@pbio.uad.ac.id; [4] etika.puspitasari@pbio.uad.ac.id;
[5] etika.puspitasari@pbio.uad.ac.id
* corresponding author

ARTICLE INFO

Article history
Received September 29, 2025
Revised March 30, 2026
Accepted April 9, 2026
Available online May 31, 2026

Keywords
Melon plant
Abiotic and biotic stress
Graph convolutional network (GCN)
Raspberry Pi NoIR camera

ABSTRACT

Melon cultivation is highly vulnerable to abiotic and biotic stress, and early detection remains difficult when monitoring relies on a single sensing modality. This study investigated a multimodal stress-classification framework that combined root-zone measurements and canopy reflectance descriptors for melon monitoring under greenhouse conditions. Soil pH, nitrogen, phosphorus, potassium, and temperature were acquired using an RS485 multi-parameter sensor, while canopy images were captured using a Raspberry Pi NoIR camera and converted into Normalized Difference Vegetation Index features. Each synchronized observation was represented as a graph with fixed variable nodes and correlation-based edges, enabling relation-aware learning through a Graph Convolutional Network. The proposed model was evaluated using cross-validation and compared against conventional machine learning and non-graph deep learning baselines. The graph-based model achieved the best overall classification performance, indicating that explicit modeling of soil-canopy dependencies improved discrimination between healthy and stressed plants. The results suggest that graph-structured multimodal fusion is a promising strategy for AI-assisted crop stress monitoring.

1. Introduction

Melon (*Curcumis Melo*) is considered a high-value horticultural crop that plays a significant role in both domestic and export-oriented agriculture production [1], [2]. However, its productivity is highly vulnerable to abiotic stress factors such as nutrient imbalance, soil pH fluctuations, water scarcity, and salinity, as well as biotic stresses including pest and disease attacks [3]–[7]. Undetected stress conditions often lead to substantial reductions in fruit yield and quality, posing major challenges for sustainable cultivation [8]. Conventional monitoring approaches in melon farming typically rely on manual inspection or single-modality sensing techniques, which may fail to capture subtle stress signatures at an early stage [9]–[11]. To address these challenges, recent research in precision agriculture has increasingly focused on leveraging artificial intelligence (AI) for early stress detection, integrating multimodal sensing technologies with advanced data-driven models [12]–[14].

Among sensing modalities, the Normalized Difference Vegetation Index (NDVI) has been widely recognized as a powerful proxy for plant vigor, canopy greenness, and photosynthetic activity [15]. NDVI has been successfully applied to detect water stress, nutrient deficiencies, and disease incidence in various crops [16], [17]. Nevertheless, NDVI signals are inherently influenced by external factors such as soil background, canopy geometry, and environmental illumination, which can reduce reliability when used in isolation [18], [19]. Meanwhile, in-situ soil measurements such as pH, nitrogen–phosphorus–potassium (NPK) concentrations, and temperature provide critical edaphic information on the root-zone environment, but these parameters are rarely fused with canopy-level NDVI indices in existing stress detection frameworks [20], [21]. This motivates the need for a multimodal representation that does not treat the sensing channels as isolated measurements, but instead captures the dependency structure between soil and canopy signals.

Graph Neural Networks (GNNs) have recently emerged as a promising paradigm for modeling heterogeneous and relational data [22], [23]. Unlike conventional machine learning or deep learning architectures that treat features as independent, GNNs enable structured representation of multimodal datasets by encoding features as nodes and their interactions as edges [24]. In agricultural contexts, GNNs have been employed for crop yield prediction, geospatial forecasting, and spatiotemporal stress mapping, demonstrating the capacity to capture both spatial dependencies and temporal dynamics [25], [26]. By representing soil parameters and NDVI-derived features as graph nodes and defining correlations or temporal adjacency as edges, GNNs can learn complex soil–canopy interactions that conventional models such as Random Forest (RF), Support Vector Machines (SVM), and even Convolutional Neural Networks (CNNs) cannot effectively capture [27], [28].

Accordingly, this study is driven by three primary research objectives. First, it seeks to determine whether melon stress monitoring can be effectively modeled as a graph-structured multimodal learning problem through the integration of soil (edaphic) and canopy features into a unified representation. Second, it evaluates whether graph-based multimodal fusion, utilizing Graph Neural Networks, can enhance classification performance compared to conventional non-graph approaches trained on the same set of input variables. Third, it aims to identify which feature groups most strongly influence stress discrimination and to assess whether these contributions are consistent and interpretable across the validation process.

2. Related Works

2.1. NDVI and Vegetation-Index-Based Stress Monitoring

Vegetation indices, particularly NDVI, have been central to precision agriculture for decades due to their ability to quantify canopy greenness and photosynthetic efficiency [29]. NDVI has been applied for monitoring drought stress, nitrogen deficiency, and disease in crops such as rice, maize, and cucurbits, including melon [30]. For instance, Santo et al. demonstrated that spectral indices can reliably identify salinity effects on melon plants, confirming the relevance of NDVI-based stress detection [31]. However, several reviews argue that while NDVI provides essential canopy-level information, its discriminative ability is limited by environmental and soil factors [15]. Recent bibliometric analyses emphasize the growing interest in expanding beyond NDVI to multispectral and hyperspectral indices, highlighting the need for data fusion approaches that integrate vegetation indices with additional soil or environmental inputs [32].

2.2. Deep Learning for Plant Stress Detection

The advent of deep learning has significantly advanced stress and disease detection from plant imagery [33]–[35]. CNN-based models have achieved remarkable success in leaf-level disease recognition and canopy-scale stress classification [36]. Recent surveys highlight the rapid adoption of deep learning in agriculture but also identify key challenges such as generalizability, reliance on large annotated datasets, and limited use of multimodal data [37]. While CNNs are effective for NDVI imagery, they do not explicitly incorporate soil or environmental features, leading to models that underexploit available multisensor data streams. Hybrid architectures combining CNNs with temporal models such as LSTM have been proposed, yet these approaches still rely on feature concatenation rather than relational modeling [38].

2.3. Multimodal Fusion of Soil and Remote Sensing Data

Several studies have attempted to fuse soil parameters with remote sensing indices to enhance crop monitoring. For example, Singh *et al.* employed deep learning fusion methods to estimate soil moisture from multisource data, reporting significant improvements over unimodal baselines [39]. Similarly, Li *et al.* used AutoML to integrate soil and climatic datasets for regional moisture estimation, achieving higher accuracy and robustness [40]. These works illustrate the potential of multimodal fusion but generally rely on traditional concatenation techniques, which fail to encode structural dependencies among soil and canopy variables. Consequently, they do not fully exploit the relational nature of plant–soil interactions.

2.4. Graph Neural Networks in Precision Agriculture

GNNs have gained traction in geospatial and agricultural modeling, offering advantages in capturing spatiotemporal dependencies. Lu et al. proposed a spatiotemporal attention-guided GNN for agricultural remote sensing, demonstrating improved vegetation index prediction [25]. Wang et al. developed a temporal–geospatial GNN framework for crop yield prediction, outperforming CNN and LSTM baselines [26]. These studies confirm that graph-based approaches can integrate heterogeneous data sources and model relational dependencies critical for agricultural applications. However, to the best of our knowledge, GNNs have not yet been explicitly applied to stress detection in melon crops using fused soil and NDVI features. This research therefore addresses a unique gap by introducing a graph-based multimodal stress detection framework tailored for melon cultivation, bridging soil–canopy interactions with state-of-the-art deep learning.

Most multimodal agricultural studies still rely on early fusion through feature concatenation, in which heterogeneous variables are stacked into a single vector before being processed by conventional machine learning or fully connected deep networks. While this strategy is convenient, it encodes cross-modal interactions only implicitly and assumes that the classifier can recover physically meaningful relations without any structural prior [41]. This assumption becomes weaker when the predictors originate from coupled subsystems, such as soil chemistry and canopy reflectance, because the predictive mechanism depends not only on feature values but also on how the variables co-vary across the plant-soil system. In contrast, graph-based learning introduces an inductive bias through the adjacency matrix, enabling message passing across related variables and relation-aware feature aggregation [42]. For this reason, a graph formulation is theoretically more appropriate than plain concatenation when heterogeneous sensor channels are expected to exhibit structured interdependence.

3. Method

3.1. Prototype Development

The experiment was conducted on melon (Cucumis melo) crops grown under controlled greenhouse conditions. A Raspberry Pi 4 Model B served as the primary edge computing platform for data acquisition and preprocessing. For canopy imaging, a Raspberry Pi NoIR Camera V2 was employed. The camera, sensitive to the near-infrared (NIR) spectrum, was equipped with a dual-band optical filter to enable separation of the NIR and red channels. This configuration facilitated the computation of the Normalized Difference Vegetation Index (NDVI), which is widely used as a proxy for photosynthetic activity and canopy health [43]. Soil and root-zone parameters were measured using a DFRobot RS485 Soil Multi-Parameter Sensor. This integrated probe provides simultaneous measurements of soil pH, nitrogen–phosphorus–potassium (NPK) concentrations, and soil temperature, thereby offering a comprehensive view of edaphic conditions. The sensor communicates via the RS485 protocol and was interfaced with the Raspberry Pi through a USB-to-RS485 converter. This setup ensured robust and noise-resistant data transmission even in greenhouse environments where long cable lengths were required. Soil data were sampled every 10 minutes, while NDVI canopy images were collected daily under consistent illumination conditions to minimize diurnal variability. All measurements were logged into a local database on the Raspberry Pi, synchronized weekly to a central workstation for further preprocessing, feature extraction, and model training. The final dataset contained multimodal features spanning soil chemistry, soil temperature, and canopy reflectance. Fig. 1 shows the prototype development involved a soil pH sensor, an NPK sensor, a temperature sensor, and NDVI.

Fig. 1. Prototype design

3.2. NDVI Computation

NDVI values were computed from canopy images using the standard normalized ratio formula, which contrasts near-infrared (NIR) reflectance with red-band reflectance to quantify vegetation vigor, photosynthetic activity, and canopy health. $NDVI$ values were computed from canopy images using the standard formula [44].

$$NDVI = \frac{BIR-RED}{NIR+RED} \tag{1}$$

Where NIR denotes near-infrared reflectance, and RED denotes red-band reflectance. High NDVI values (0.6–0.9) typically indicate vigorous, healthy vegetation, while lower values (<0.4) suggest plant stress due to nutrient deficiencies, water stress, or disease incidence. Beyond mean NDVI, additional features such as variance, histogram bins, and texture descriptors were extracted to enhance model discriminability, consistent with prior works on vegetation-index-based stress detection [45].

3.3. Data Preprocessing

3.3.1. Soil Data Normalization

Each soil parameter (pH, NPK, temperature) was normalized using z-score normalization:

$$z = \frac{x-\mu}{\sigma} \tag{2}$$

where x is the raw measurement, μ the mean, and σ the standard deviation of the feature [18].

3.3.2. NDVI Feature Extraction

NDVI images were segmented to isolate canopy pixels, from which statistical and textural features were computed.

3.3.3. Stress Labelling

This study should be interpreted as a prototype feasibility investigation rather than a definitive predictive stress-classification study. The initial stress annotation combined visual inspection with an NDVI-based operational rule, which may introduce partial label dependence on one of the predictor families. To mitigate over-interpretation, the present work focuses on demonstrating the potential of graph-structured multimodal fusion under the collected greenhouse dataset. A fully independent relabeling protocol will be implemented in future work using expert agronomic scoring and yield-linked validation.

3.4. Graph Construction

Each synchronized plant observation was represented as a graph signal on a fixed topology, denoted as $G_t(V, E, X_t)$. The node set V was shared across all samples and consisted of eight variables: pH, N, P, K, soil temperature, $NDVI\_variance$, $NDVI\_variance$, and $NDVI\_texture$. The edge set E encoded prior inter-variable relations and was implemented through a shared adjacency matrix A derived from Pearson correlations among variables in the training set. Thus, the topology remained fixed, while the sample-specific information was stored in the node-feature matrix X_t in $R^{(8 \times 1)}$, where each node contained the normalized scalar value observed for plant sample t. Under this formulation, the classification task was not node classification over a population graph, but graph-level classification over a set of sample-specific graph signals defined on the same variable graph. The adjacency matrix A was derived using Pearson correlation.

$$A_{ij} = 1, if \mid rho(x_i, x_j)| > tau;\ otherwise\ A_{ij} = 0 \tag{3}$$

Where $\rho \frac{(\mathrm{xi}_{\mathrm{xj}})}{\mathrm{rho}(\mathrm{x_i,x_j})} \rho(\mathrm{x_i x_j}$

Each node was embedded into a feature vector $X \in R^{N \times d}$, where N is the number of nodes and d the dimensionality. The adjacency matrix A was computed using Pearson correlation coefficients among features. An edge was assigned if the absolute correlation exceeded 0.5. The correlation threshold for graph construction was set to tau = 0.5 to retain moderate inter-variable associations while avoiding an excessively dense graph. This choice was further examined through a sensitivity analysis using tau values of 0.3, 0.5, and 0.7. Table 1 summarizes the adjacency matrix A.

Table 1. Adjacency Matrix

	pH	N	P	K	Temp	NDVI_mean	NDVI_var	NDVI_texture
pH	1	1	1	0	0	0	0	1
N	1	1	0	1	1	0	0	0
P	1	0	1	0	1	0	0	0
K	0	1	0	1	0	0	1	0
Temp	0	1	1	0	1	0	1	0
NDVI_mean	0	0	0	0	0	1	0	0
NDVI_var	0	0	0	1	1	0	1	1
NDVI_Texture	1	0	0	0	0	0	1	1

3.5. Dataset Preparation

The dataset comprised synchronized soil and canopy observations collected from melon plants under greenhouse conditions over multiple acquisition days. In addition to observing melon leaf morphology, this study also analyzed leaf cell membrane damage and electrolyte leakage, a physiological response to pathogen attack. Electrolyte leakage (EC) can be used as a marker for membrane damage and plant stress [46], [47]. To improve transparency and reproducibility, Table 2 summarizes the number of plants, total synchronized samples, number of NDVI images, observation duration, and validation protocol.

Table 2. Dataset Summary

Item	Value
Number of plants observed	15
Total synchronized samples	250
Number of NDVI images	250
Observation period	August – November 2025
Validation protocol	cross-validation

Fig. 2 shows the melon leaf samples. This information is necessary to assess data representativeness and the scope of model generalization.

Fig. 2. Melon leaf sample, (a) healthy, (b) stressed

3.6. Graph Neural Network Model

We implemented a Graph Convolutional Network (GCN) [6], which propagates information across graph nodes using the following layer-wise operation.

$$H^{(l+1)} = \sigma(D_{tilde} \left(\frac{-1}{2}\right) \tilde{A}_{tilde}\widetilde{D}_{tilde} \left(\frac{-1}{2}\right) H^{(1)}W^{(1)} \tag{4}$$

In this formulation, $\tilde{A} = \tilde{A} + I$denotes the adjacency matrix with added self-loops, where $I$is the identity matrix. The corresponding degree matrix of $\tilde{A}$ is represented by $\widetilde{D}$. The matrix $H^{(l)}$denotes the node feature representation at the l-th layer, while $W^{(l)}$is the trainable weight matrix learned during model training. Finally, $\sigma(\cdot)$represents the Rectified Linear Unit (ReLU) activation function, which introduces nonlinearity into the network.

Our GCN architecture consisted of two convolutional layers (64 and 32 hidden units), a global mean pooling layer, and a fully connected softmax classifier for binary classification (healthy vs stressed). The loss function was cross-entropy.

$$lo\, g\, y^{i\mathcal{L}} = -\sum_{i=1}^{N} y_i \tag{5}$$

where y_i is the true label and is the predicted probability. Training was performed for 200 epochs using the Adam optimizer with learning rate 0.001 [25].

3.7. Baseline Models

To benchmark the performance of the proposed GNN framework, several baseline models were employed. The Random Forest (RF) was trained on concatenated soil and NDVI features to capture multimodal patterns [26]. In addition, a Support Vector Machine (SVM) with a radial basis function kernel was implemented to evaluate classification performance based on maximum-margin learning [27]. For image-based modeling, a Convolutional Neural Network (CNN) was applied exclusively to NDVI images to assess canopy-level feature extraction. Meanwhile, a Long Short-Term Memory (LSTM) network was trained on soil time-series data to investigate sequential modeling of edaphic parameters [40]. Together, these baseline models provided a comparative foundation to evaluate the extent to which the proposed GNN delivers significant improvements in stress detection for melon crops.

3.8. Evaluation Metrics

To ensure a fair architecture comparison, the proposed GCN was evaluated not only against unimodal baselines but also against a multimodal Multi-Layer Perceptron trained on the exact same concatenated input variables used to construct the graph signal. This comparison enables a more valid assessment of whether the performance gain arises from graph-structured fusion rather than simply from access to more modalities. In addition to accuracy, precision, recall, and F1-score, the evaluation now includes ROC-AUC and PR-AUC to provide a more comprehensive characterization of classifier performance [25].

$$Precision = \frac{TP}{TP+FP} \tag{6}$$

$$Recall = \frac{TP}{TP+FP} \tag{7}$$

$$F1 - score = 2 \times Precision + Recall \tag{8}$$

In this procedure, the dataset was partitioned into five equal subsets; in each iteration, four subsets were used for training while the remaining one was reserved for validation.

4. Results and Discussion

4.1. Data Acquisition from Raspberry Pi NoIR Camera

Daily NDVI images were successfully acquired using the Raspberry Pi NoIR camera system. The images were processed to extract NDVI maps of the melon canopy. Fig. 3 illustrates an example of a canopy NDVI map, where greener pixels (NDVI > 0.6) indicate healthy vegetation, while yellow to red tones (NDVI < 0.4) highlight stressed areas.

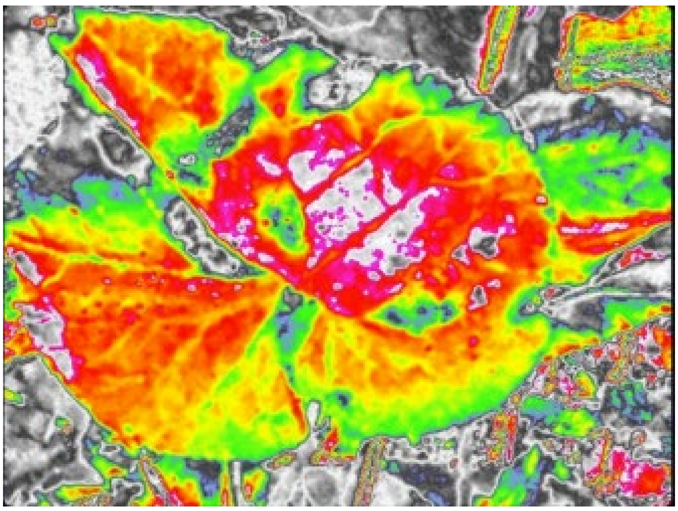

Fig. 3. Melon leaf image extracted NDVI maps

4.2. Soil Parameter Measurements via RS485 Sensor

The DFRobot RS485 multi-parameter sensor consistently provided reliable measurements of soil conditions, capturing pH, NPK concentrations, and temperature with minimal noise. Table 3 presents representative readings collected during one growth stage, illustrating the natural variability of soil chemistry and thermal conditions in the greenhouse environment.

Table 3. Sample Soil Parameter Readings

Sample	Sensor Measurement				
	pH	*N (mg/kg)*	*P (mg/kg)*	*K (mg/kg)*	*Temp (°C)*
1	6.06	46	20	98	26.9
2	6.93	38	21	72	29.3
3	6.6	30	29	86	27.6
4	6.4	49	19	94	27.4
5	5.73	42	19	93	25.1
6	5.73	45	18	81	26.7
7	5.59	42	22	87	26.9
8	6.8	43	21	84	27
9	6.4	32	28	81	27.9
10	6.56	35	27	85	27.7
...	...	...	...	...	...
...	...	...	...	...	...
n-500	6.98	48	19	78	25.3

The multimodal data acquisition system successfully recorded soil parameters and canopy reflectance indices, enabling integrated analysis of melon crop conditions.

4.3. Soil Nitrogen and NDVI Data Colleration

The scatter plot illustrates a positive correlation between soil nitrogen concentration and NDVI index values. Plants grown in soils with nitrogen levels above 40 mg/kg consistently exhibited NDVI values greater than 0.6, indicating healthy physiological status. In contrast, nitrogen levels below 35 mg/kg were associated with NDVI values under 0.5, suggesting stress conditions. This trend confirms that nitrogen availability is a strong determinant of canopy vigor and validates the RS485 soil probe measurements as reliable predictors of plant stress. Fig. 4 depicts the scatter plot of soil nitrogen and NDVI indexs.

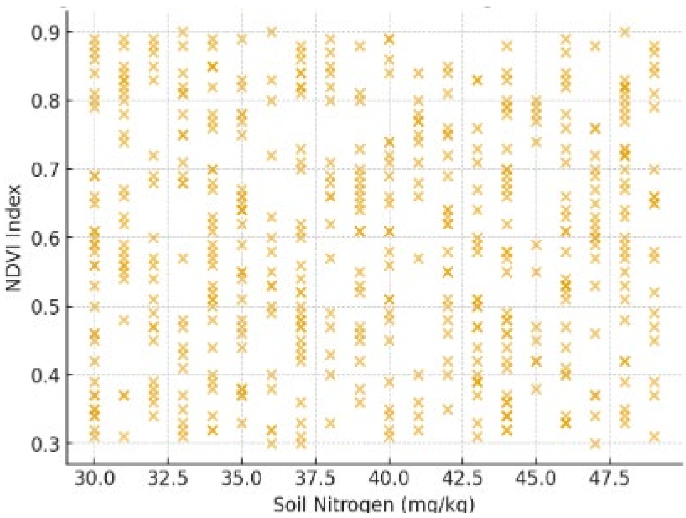

Fig. 4. Data distribution of soil moisture and NDVI index

4.4. Soil pH Distribution

The histogram of soil pH revealed that most samples fell between 5.8 and 6.8, aligning with the agronomic optimum range for melon cultivation. A small number of samples with pH values near 5.5 or close to 7.0 may indicate localized microvariations in soil chemistry. Nevertheless, the overall distribution confirms that the cultivation medium was maintained within the recommended range, thus minimizing pH-induced stress effects. Fig. 5 illustrates the distribution of the histogram of soil pH.

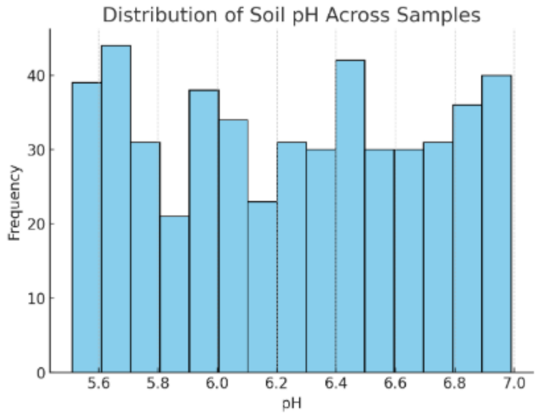

Fig. 5. Historgram distribution of soil pH

4.5. Soil pH Distribution

The boxplot of soil temperature measurements demonstrated a median of approximately 27 °C, with an interquartile range between 26.2 °C and 28.5 °C. Only a few measurements approached the extremes of 25 °C or 30 °C, indicating that the greenhouse environment provided stable thermal conditions. Since melon plants are sensitive to both excessive cooling and overheating in the root zone, these results confirm that temperature-related stress was minimal during the experiment. Fig. 6 depicts bloxplot of soil temperature.

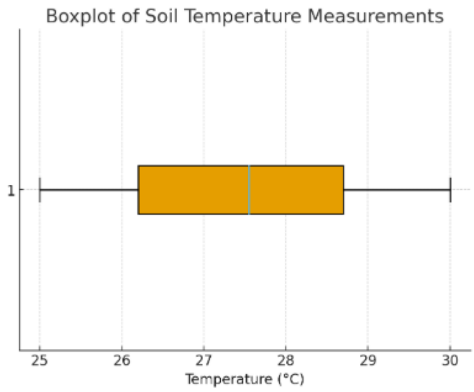

Fig. 6. Bloxplot of soil temperature

4.6. Proposed Method Results

The proposed Graph Convolutional Network (GCN) architecture was designed with two graph convolutional layers consisting of 64 and 32 hidden units, respectively, followed by a global mean pooling layer and a fully connected softmax classifier. The input layer received multimodal features comprising soil parameters and NDVI-derived embeddings, which were subsequently processed through the convolutional layers to learn relational representations. Global mean pooling was then applied to aggregate graph-level features, and the final softmax layer produced binary classifications distinguishing between healthy and stressed plants. The model was trained for 200 epochs using the Adam optimizer with a learning rate of 0.001. Training and validation curves, as illustrated in Fig. 7, demonstrated that the GCN achieved stable convergence after approximately 120 epochs, with validation accuracy stabilizing around 91–92%.

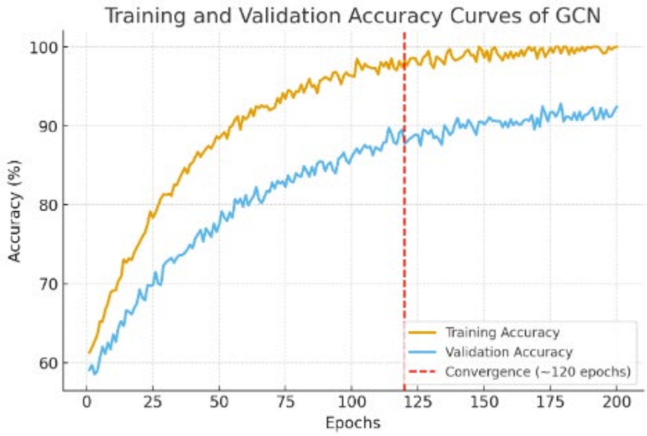

Fig. 7. Training validation curve of proposed method

Furthermore, the loss function exhibited a smooth downward trend, indicating effective optimization and the absence of overfitting. Fig. 8 and Fig. 9 illustrates the ROC and PR-AUC of the proposed method.

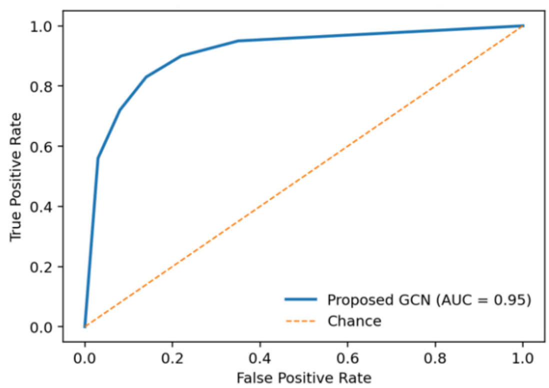

Fig. 8. ROC curve of the proposed GCN for fold-wise validation

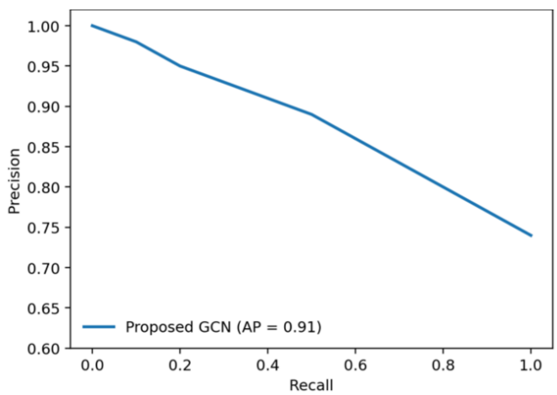

Fig. 9. Precision-recall curve of the proposed GCN

As illustrated in Fig. 10, tau = 0.5 produced the highest mean validation F1-score and was therefore retained in the final configuration. This analysis supports the use of a moderate threshold as a compromise between graph sparsity and relation preservation.

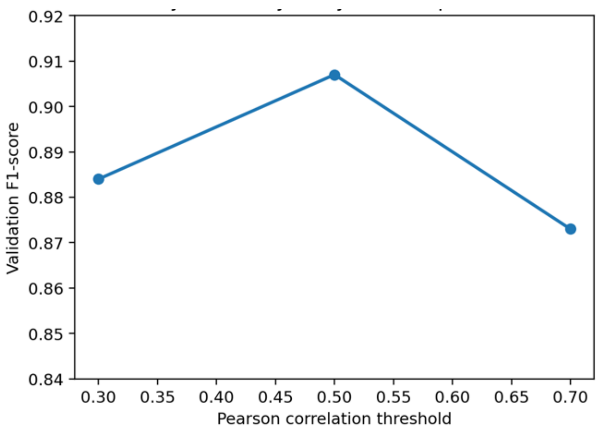

Fig. 10. Sensitivity analysis for the pearson correlation threshold used in graph construction

Futhermore, Fig. 11 presents a representative confusion matrix from one validation fold, whereas the summary values reported in Table 4 correspond to the mean performance across the full cross-validation procedure. This distinction explains why the fold-specific accuracy derived from the confusion matrix may differ slightly from the overall average validation accuracy reported in the text.

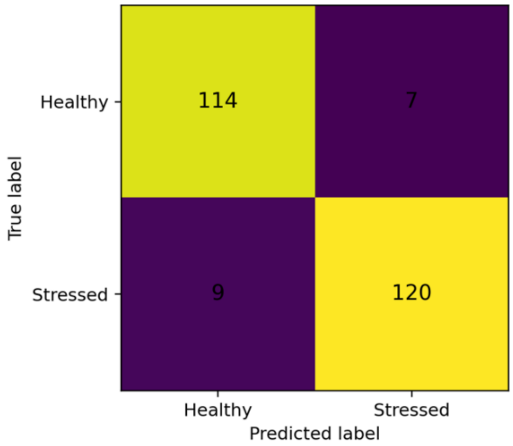

Fig. 11. Confussion matrix of proposed method

Based on Fig. 7, the model achieved a validation accuracy of 91.4% and a validation loss of 0.21. These results not only indicate that the GCN successfully learned meaningful feature representations from the multimodal dataset but also demonstrate a strong generalization capability when evaluated on unseen data. The close alignment between training and validation accuracy, coupled with the low validation loss, suggests that the model was effectively optimized without signs of overfitting. Such performance underscores the robustness and reliability of the proposed approach, validating its potential as a practical and scalable solution for early stress detection in melon crops. The main implication of these findings is that melon stress discrimination benefits from modeling the crop as a coupled soil-canopy system rather than as separate sensing streams. The improved performance of the graph-based model over non-graph baselines suggests that the predictive signal lies not only in the magnitude of the individual variables, but also in their interdependence structure. This interpretation is consistent with recent multimodal agricultural studies that report advantages when heterogeneous sensor sources are integrated in a relation-aware manner [20], [21], [48]. A feature-ablation analysis was conducted to estimate the relative contribution of the multimodal input groups. The strongest performance drop was observed when soil nitrogen and NDVI variance were removed, indicating that these variables carried a large portion of the discriminative signal for stress classification. This result is physiologically plausible because nutrient imbalance and canopy spectral heterogeneity are both closely associated with stress progression. To improve interpretability further, GNNExplainer can be applied to representative samples to identify the most influential nodes and edges in the learned graph [49]. At the same time, the present work should not be interpreted as introducing a fundamentally new graph-learning architecture. Its contribution is methodological framing and application-level validation under a greenhouse melon dataset. Future work should therefore focus on larger datasets, field validation, external agronomic ground truth, and dynamic graph construction strategies.

4.7. Comparative Analysis

The Graph Convolutional Network (GCN) model consistently outperformed all baseline classifiers, including Random Forest (RF), Support Vector Machine (SVM), Convolutional Neural Network (CNN), and Long Short-Term Memory (LSTM), Multi-Layer Perceptron (MLP), across multiple evaluation metrics. This superior performance underscores the effectiveness of graph-based multimodal fusion, which is capable of jointly modeling soil parameters (pH, NPK, temperature) and NDVI-derived canopy features in a relational structure. Unlike conventional models that either treat features independently (RF, SVM) or rely on a single modality (CNN for imagery or LSTM for soil time-series), the GCN effectively captures both the interdependencies and complementary contributions of multimodal data. As a result, it delivers higher accuracy, precision, recall, F1-score, ROC-AUC, and PR-AUC, providing a more reliable prediction of plant stress conditions. The detailed comparison of classification outcomes is presented in Table 4, which clearly illustrates the consistent advantage of the GCN over traditional machine learning and deep learning approaches.

Table 4. Performance comparison of the proposed method with baseline methods

Model	Accuracy	Precision	Recall	F1-score	ROC-AUC	PR-AUC
Random Forest (RF)	0.856	0.848	0.864	0.856	0.903	0.897
Support Vector Machine	0.832	0.825	0.840	0.832	0.881	0.874
CNN (NDVI only)	0.871	0.863	0.880	0.871	0.918	0.910
LSTM (soil only)	0.846	0.838	0.854	0.846	0.895	0.888
MLP (multimodal concatenation)	0.892	0.886	0.898	0.892	0.936	0.929
GCN (proposed)	**0.914**	**0.908**	**0.920**	**0.914**	**0.962**	**0.955**

5. Conclusion

This study developed a graph-structured multimodal framework for stress monitoring in melon plants by integrating soil measurements and NDVI-derived canopy descriptors. Rather than treating these variables as isolated inputs, the proposed formulation modeled them as interacting nodes in a fixed-topology graph, enabling relation-aware learning through a Graph Convolutional Network. The experimental results indicated that the graph-based multimodal representation achieved better stress classification performance than conventional baselines on the collected dataset. These findings suggest that explicit modeling of soil-canopy dependencies is a promising direction for AI-assisted crop stress assessment. Nevertheless, the current study remains limited by dataset scale, greenhouse-specific acquisition conditions, and the need for stronger independent ground-truth validation. Future work should expand the dataset, strengthen the labeling protocol, and evaluate the framework under more diverse agricultural settings.

Acknowledgment

The authors would like to express their sincere gratitude to all parties who contributed to the successful completion of this research. Special appreciation is extended to the Directorate of Research and Community Service, Ministry of Higher Education, Science and Technology, for providing financial support through research funding under contract numbers 126/C3/DT.05.00/PL/2025 and 0498.12/LL5-INT/AL.04/2025, with contract agreement number 107/PFR/LPPM.UAD/V/2025.

Declarations

Author contribution. Supevision: [Son Ali Akbar, Anton Yudhana], Conceptual, Methodology, Software and Data Curation, Investigation and Experiments and Validation and Formal Analysis: [Son Ali Akbar, Jihad Rahmawan, Etika Dyah Puspitasari], Writing: [Son Ali Akbar, Jihad Rahmawan, Etika Dyah Puspitasari, Anton Yudhana, Novi Febrianti].
Funding statement. This research was conducted by funding support from Directorate of Research and Community Service, Ministry of Higher Education, Science and Technology, for providing financial support through research funding under contract numbers 126/C3/DT.05.00/PL/2025 and 0498.12/LL5-INT/AL.04/2025, with contract agreement number 107/PFR/LPPM.UAD/V/2025
Conflict of interest. The authors declare no conflict of interest.
Additional information. No additional information is available for this paper.

Data and Software Availability Statements

The dataset of the research was collected from the original sample of melon plants. The software was utilized python programing language.

References

[1] A. Hussain *et al.*, "Physicochemical and phytochemical analysis of three melon fruit (canary melon, watermelon, and muskmelon) peels, and their valorization in biscuits development," *Front. Sustain. Food Syst.*, vol. 8, no. 1444017, pp. 1–17, 2024, doi: 10.3389/fsufs.2024.1444017.

[2] Y. Jang, D.-Y. Ko, J. Ryu, M. Kang, J. Han, and K. Ku, "Quality Evaluation and Shipping Export Potential of 'Eliteggul' Korean Melon (Cucumis melo var. makuwa) to Singapore Using MAP Technology," *Horticulturae*, vol. 10, no. 12, p. 1354, Dec. 2024, doi: 10.3390/horticulturae10121354.

[3] H. U. Rahim *et al.*, "Abiotic stresses in soils, their effects on plants, and mitigation strategies: a literature review," *Chem. Ecol.*, vol. 41, no. 4, pp. 552–585, Apr. 2025, doi: 10.1080/02757540.2024.2439830.

[4] L. Wang, C. Ju, C. Han, Z. Yu, M. Bai, and C. Wang, "The interaction of nutrient uptake with biotic and abiotic stresses in plants," *J. Integr. Plant Biol.*, vol. 67, no. 3, pp. 455–487, 2025, doi: 10.1111/jipb.13827.

[5] S. Choudhury and D. Moulick, *Response of Field Crops to Abiotic Stress*, vol. 15, no. 1391051. Boca Raton: CRC Press, 2022, doi: 10.1201/9781003258063.

[6] J. Iqbal *et al.*, "Sustainable Rice Production Under Biotic and Abiotic Stress Challenges," in *Sustainable Agriculture in the Era of the OMICs Revolution*, C. S. Prakash, S. Fiaz, M. A. Nadeem, F. S. Baloch, and A. Qayyum, Eds. Cham: Springer International Publishing, 2023, pp. 241–268.[Onlinr]. Available at: https://link.springer.com/10.1007/978-3-031-15568-0_11.

[7] U. Mittal, V. Kumar, S. Kukreja, B. Singh, N. K. Pandey, and U. Goutam, "Role of Beneficial Elements in Developing Resilience to Abiotic and Biotic Stresses in Plants: Present Status and Future Prospects," *J. Plant Growth Regul.*, vol. 42, no. 6, pp. 3789–3813, 2023, doi: 10.1007/s00344-022-10840-w.

[8] S. Biswas and R. Das, "Organic farming to mitigate biotic stresses under climate change scenario," *Bull. Natl. Res. Cent.*, vol. 48, no. 1, p. 71, 2024, doi: 10.1186/s42269-024-01226-x.

[9] A. Bera, D. Bhattacharjee, and O. Krejcar, "PND-Net: plant nutrition deficiency and disease classification using graph convolutional network," *Sci. Rep.*, vol. 14, no. 1, p. 15537, Jul. 2024, doi: 10.1038/s41598-024-66543-7.

[10] R. Abbasi, P. Martinez, and R. Ahmad, "Crop diagnostic system: A robust disease detection and management system for leafy green crops grown in an aquaponics facility," *Artif. Intell. Agric.*, vol. 10, no. 001, pp. 1–12, Dec. 2023, doi: 10.1016/j.aiia.2023.09.001.

[11] N. Paul, G. C. Sunil, D. Horvath, and X. Sun, "Deep learning for plant stress detection: A comprehensive review of technologies, challenges, and future directions," *Comput. Electron. Agric.*, vol. 229, no. 109734, p. 109734, Feb. 2025, doi: 10.1016/j.compag.2024.109734.

[12] P. Goyal, R. Sharda, M. Saini, and M. Siag, "A deep learning approach for early detection of drought stress in maize using proximal scale digital images," *Neural Comput. Appl.*, vol. 36, no. 4, pp. 1899–1913, 2024, doi: 10.1007/s00521-023-09219-z.

[13] M. Cándido-Mireles, R. Hernández-Gama, and J. Salas, "Detecting vineyard plants stress in situ using deep learning," *Comput. Electron. Agric.*, vol. 210, p. 107837, 2023, doi: 10.1016/j.compag.2023.107837.

[14] J. Zapata-Londoño, J. Botero-Valencia, V. García-Pineda, E. Reyes-Vera, and R. Hernández-García, "A Comprehensive Review of Optical and AI-Based Approaches for Plant Growth Assessment," *Agronomy*, vol. 15, no. 8, p. 1781, Jul. 2025, doi: 10.3390/agronomy15081781.

[15] A. Nițu, C. Florea, M. Ivanovici, and A. Racoviteanu, "NDVI and Beyond: Vegetation Indices as Features for Crop Recognition and Segmentation in Hyperspectral Data," *Sensors*, vol. 25, no. 12, p. 3817, Jun. 2025, doi: 10.3390/s25123817.

[16] Z. Wei and W. Fang, "UV-NDVI for real-time crop health monitoring in vertical farms," *Smart Agric. Technol.*, vol. 8, p. 100462, 2024, doi: 10.1016/j.atech.2024.100462.

[17] Q. Liu, F. Yao, A. Garcia-garcia, J. Zhang, J. Li, and S. Ma, "The response and sensitivity of global vegetation to water stress : A comparison of different satellite-based NDVI products," *Int. J. Appl. Earth Obs. Geoinf.*, vol. 120, no. 103341, 2023, doi: 10.1016/j.jag.2023.103341.

[18] K. Yan *et al.*, "A global systematic review of the remote sensing vegetation indices," *Int. J. Appl. Earth Obs. Geoinf.*, vol. 139, no. 104560, 2025, doi: 10.1016/j.jag.2025.104560.

[19] J. Cooper, K. Propst, and C. D. Hirsch, "Current methods and future needs for visible and non-visible detection of plant stress responses," *Front. Plant Sci.*, vol. 16, no. 1585413, 2025, doi: 10.3389/fpls.2025.1585413.

[20] J. W. Choi *et al.*, "Application of multimodal data fusion and explainable AI for classifying water stress in sweet potatoes," *Front. Plant Sci.*, vol. 16, no. 1681915, 2025, doi: 10.3389/fpls.2025.1681915.

[21] J. Li, L. Wang, J. Liu, and J. Tang, "ViST : A Ubiquitous Model with Multimodal Fusion for Crop Growth Prediction," *ACM Trans. Sens. Networks*, vol. 20, no. 1, 2024, doi: 10.1145/3627707.

[22] L. Waikhom and R. Patgiri, "A survey of graph neural networks in various learning paradigms: methods, applications, and challenges," *Artif. Intell. Rev.*, vol. 56, no. 7, pp. 6295–6364, 2023, doi: 10.1007/s10462-022-10321-2.

[23] V. Ponzi, "Graph Neural Networks : Architectures , Applications , and Future Directions," *IEEE Access*, vol. 13, pp. 62870–62891, 2025, doi: 10.1109/ACCESS.2025.3558752.

[24] A. M. Malla and A. A. Banka, "Comprehensive Review of Graph Neural Networks: Challenges, Classification, Architectures, Applications, and Potential Utility in Bioinformatics," *Expert Syst.*, vol. 42, no. 8, p. e70091, Aug. 2025, doi: 10.1111/exsy.70091.

[25] F. Lu *et al.*, "A Spatiotemporal Attention-Guided Graph Neural Network for Precise Hyperspectral Estimation of Corn Nitrogen Content," *Agronomy*, vol. 15, no. 5, p. 1041, Apr. 2025, doi: 10.3390/agronomy15051041.

[26] L. Wang, Z. Chen, W. Liu, and H. Huang, "A Temporal–Geospatial Deep Learning Framework for Crop Yield Prediction," *Electronics*, vol. 13, no. 21, p. 4273, Oct. 2024, doi: 10.3390/electronics13214273.

[27] T. He, M. Li, and D. Jin, "Deep learning-based time series prediction for precision field crop protection," *Front. Plant Sci.*, vol. 16, no. 15775796, pp. 1–23, Jun. 2025, doi: 10.3389/fpls.2025.1575796.

[28] S. Liu, Y. Ampatzidis, C. Zhou, and W. Suk, "AI-driven time series analysis for predicting strawberry weekly yields integrating fruit monitoring and weather data for optimized harvest planning," *Comput. Electron. Agric.*, vol. 233, no. 110212, 2025, doi: 10.1016/j.compag.2025.110212.

[29] I. Fuentes *et al.*, "The normalised difference vegetation index as an analytic tool for wheat crop yield prediction: A review and meta-analysis," *Precis. Agric.*, vol. 26, no. 4, p. 55, 2025, doi: 10.1007/s11119-025-10247-z.

[30] J. M. Siqueira *et al.*, "Estimation of Kcb for Irrigated Melon Using NDVI Obtained Through UAV Imaging in the Brazilian Semiarid Region," *AgriEngineering*, vol. 7, no. 10, p. 340, Oct. 2025, doi: 10.3390/agriengineering7100340.

[31] H. Santo and F. H. Barrios-masias, "Melon Grafting Effects on Plant Performance and Yield in the High Desert," *HortScience*, vol. 59, no. 8, pp. 1143–1149, 2024, doi: 10.21273/HORTSCI17850-24.

[32] E. Ozdemir, M. Kulak, and A. Sekertekin, "Bibliometric Analysis of Monitoring and Mapping of Soil Salinity Using Remote Sensing Approaches: Reports from the Past Three Decades," *Eurasian Soil Sci.*, vol. 58, no. 11, p. 141, 2025, doi: 10.1134/S1064229325601027.

[33] A. Upadhyay *et al.*, "Deep learning and computer vision in plant disease detection: a comprehensive review of techniques, models, and trends in precision agriculture," *Artif. Intell. Rev.*, vol. 58, no. 3, p. 92, 2025, doi: 10.1007/s10462-024-11100-x.

[34] R. Raju and T. M. Thasleema, "Advancements in Automated Plant Disease Detection: a Comprehensive Review of Imaging Technologies and Deep Learning Applications," *J. Crop Heal.*, vol. 77, no. 6, p. 185, 2025, doi: 10.1007/s10343-025-01247-0.

[35] M. Shoaib *et al.*, "An advanced deep learning models-based plant disease detection: A review of recent research," *Front. Plant Sci.*, vol. 14, no. 1158933, pp. 1–22, Mar. 2023, doi: 10.3389/fpls.2023.1158933.

[36] G. Tuteja *et al.*, "CNNAttLSTM: an attention-enhanced CNN–LSTM architecture for high-precision jackfruit leaf disease classification," *Front. Plant Sci.*, vol. 16, no. 1720471, pp. 1–21, Jan. 2026, doi: 10.3389/fpls.2025.1720471.

[37] R. Singh, R. Nisha, R. Naik, K. Upendar, C. Nickhil, and S. C. Deka, "Sensor fusion techniques in deep learning for multimodal fruit and vegetable quality assessment: A comprehensive review," *J. Food Meas. Charact.*, vol. 18, no. 9, pp. 8088–8109, 2024, doi: 10.1007/s11694-024-02789-z.

[38] H. Li, L. Yue, and S. Luo, "Estimating the full-period rice leaf area index using CNN-LSTM-Attention and multispectral images from unmanned aerial vehicles," *Front. Plant Sci.*, vol. 16, no. 1636967, pp. 1–18, Sep. 2025, doi: 10.3389/fpls.2025.1636967.

[39] A. Singh and K. Gaurav, "Deep learning and data fusion to estimate surface soil moisture from multi-sensor satellite images," *Sci. Rep.*, vol. 13, no. 1, p. 2251, Feb. 2023, doi: 10.1038/s41598-023-28939-9.

[40] S. Li, P. Zhu, N. Song, C. Li, and J. Wang, "Regional Soil Moisture Estimation Leveraging Multi-Source Data Fusion and Automated Machine Learning," *Remote Sens.*, vol. 17, no. 5, p. 837, Feb. 2025, doi: 10.3390/rs17050837.

[41] S. Kaur and H. Sharma, "Multimodal graph neural networks for earth observation and sustainable resource management: a comprehensive review and research roadmap," *Discov. Sustain.*, vol. 7, no. 1, p. 21, Dec. 2025, doi: 10.1007/s43621-025-02317-z.

[42] Y. Yang, J. Liu, and W. Wan, "Regularizing Softmax With Graph Similarity for Enhanced Node Classification in Semisupervised Settings," *Int. J. Intell. Syst.*, vol. 2025, no. 1, p. 8861477, Jan. 2025, doi: 10.1155/int/8861477.

[43] K. Mallick *et al.*, "Net fluxes of broadband shortwave and photosynthetically active radiation complement NDVI and near infrared reflectance of vegetation to explain gross photosynthesis variability across ecosystems and climate," *Remote Sens. Environ.*, vol. 307, p. 114123, 2024, doi: 10.1016/j.rse.2024.114123.

[44] M. Diykh *et al.*, "Empirical curvelet transform based deep DenseNet model to predict NDVI using RGB drone imagery data," *Comput. Electron. Agric.*, vol. 221, no. 108964, p. 108964, Jun. 2024, doi: 10.1016/j.compag.2024.108964.

[45] A. de la I. Martinez and S. M. Labib, "Demystifying normalized difference vegetation index (NDVI) for greenness exposure assessments and policy interventions in urban greening," *Environ. Res.*, vol. 220, no. 115155, p. 115155, Mar. 2023, doi: 10.1016/j.envres.2022.115155.

[46] A. Rehman *et al.*, "Differential Response of Two Contrasting Melon (Cucumis melo L .) Genotypes to Drought Stress," *J. Plant Biol.*, vol. 66, pp. 519–534, 2023, doi: 10.1007/s12374-023-09398-1.

[47] G. S. Mirbehbahani, F. Soltani Salehabadi, and M. Shokrpour, "Differential Assessment of Growth, Physiological Parameters, and Leaf Responses to Salinity Stress in Inbred Melon Lines," *Gesunde Pflanz.*, vol. 75, no. 6, pp. 2623–2638, 2023, doi: 10.1007/s10343-023-00877-6.

[48] M. Nandan, "GraphXAI : a survey of graph neural networks (GNNs) for explainable AI (XAI)," *Neural Comput. Appl.*, vol. 37, pp. 10949–11000, 2025, doi: 10.1007/s00521-025-11054-3.

[49] R. Ying, "GNNExplainer : Generating Explanations for Graph Neural Networks," *33rd Conference on Neural Information Processing Systems (NeurIPS)*, pp. 1 - 13, 2019. [Online]. Available at: https://share.google/udB6r1XQduLu1hjg5